IEEE Access
Multidisciplinary | Rapid Review | Open Access Journal

Received December 25, 2021, accepted January 30, 2022, date of publication February 9, 2022, date of current version February 16, 2022.

*Digital Object Identifier 10.1109/ACCESS.2022.3150482*

# Influence of Conducting Particle on DC Flashover Characteristics and Tracking Property of GIS/GIL Insulator

**XIAOLONG LI, (Member, IEEE), CHEN CAO, (Member, IEEE), AND XIN LIN, (Member, IEEE)**
School of Electrical Engineering, Shenyang University of Technology, Shenyang 110870, China

Corresponding author: Xiaolong Li (xiaolongli@sut.edu.cn)

This work was supported by the National Natural Science Foundation of China under Grant 51807122 and Grant 52107157.

**ABSTRACT** Flashover at gas/insulator interface acts as a vital challenge to the safe and stable operation of gas-insulated system especially when involved with surface metallic particle. In this paper, flashover characteristics at $SF_6$/epoxy insulator interface were investigated concerning on the tracking property based on image analysis. DC flashover experiments were operated for basin-type spacer with metallic particle at various locations. Flashover voltage was obtained and tracking on the surface after successive flashover was captured. Improved image analysis method based on fractal theory was carried out to evaluate tracking pattern quantitatively. The relation between the fractal dimension of tracking and field distribution at particle tip was revealed. Obtained results showed that flashover voltage decreased due to severe field distortion with moving particle from ground to HV electrode. Meanwhile, fractal dimension of tracking covering the area from particle to ground electrode indicated centralized tendency. Simulation result confirmed this variation as the consequence of centralized field distribution at the tip of particle. The quantitative relation between fractal dimension and field distribution suggests new sight to estimate the influence of metallic particle on insulation property in the gas-insulated system.

**INDEX TERMS** Gas insulated switchgear, gas insulated transmission lines, insulator, fractal dimension, flashover, tracking, metallic particle.

## I. INTRODUCTION

Solid insulators are widely applied in gas-insulated apparatus including gas insulated switchgear (GIS) and gas insulated transmission lines (GIL) functioning as the main supporting and isolating components with insulating property [1], [2]. Then, gas/solid interface will form in the system due to the appearance of solid insulator. It is claimed that discharge would occur at the interface leading to surface flashover and finally resulting in severe operation failure to power system [3]. Further, metallic particle which may be introduced in manufacture, transportation or operation would be adhered on the insulator surface under electric field stress [4], [5]. This may cause severe field distortion and contribute to the initiation of flashover and is reported as a vital issue for the system [6]–[8].

Currently, efforts have been paid on the investigation of flashover characteristics on insulator surface [9]–[11]. It is argued that slight damage would appear on the surface with light tracking as the consequence of single flashover [12]. And single discharge follows random propagation path and develops in random directions. However, damage due to successive discharge may promote surface deterioration by providing possible propagation path for continuous discharge and finally lead to the decrease of surface strength. It is reported that carbonized tracks would remain on the surface with conducting paths attributing to the carbon element in epoxy resin [13]. Tracking indicates the propagation property of discharge and may provide potential approach to reveal the propagation and probability characteristics of surface discharge. Thus, it is meaningful to study tracking property referring to successive discharge since it relates to the flashover property during long-term operation. Actually, it is difficult to obtain flashover image directly from light emitted during discharge process via on-line technique which is

The associate editor coordinating the review of this manuscript and approving it for publication was Mohd Zainal Abidin Ab Kadir.

different from creeping discharge as reported in [14] and [15]. Tracking taken from insulator surface via off-line method performs as a possible approach to diagnose and analyses flashover characteristics.

Further, image analysis method can be applied to evaluate the tracking property. Among all the image analysis method, fractal dimension (FD) is considered to deal with discharge property concerning on filamentary structure with desirable expectation. L. Kebbabi *et al.* investigated the influence of solid insulator on creeping discharge pattern based on the calculation of fractal dimension [16]. Y. Lv *et al.* revealed the stream propagation property with the help of fractal dimension in nano-modified transformer oil [17]. Since the tracking follows the shape of the insulator, which may result in perspective to view direction in image considering the irregular shape of insulator [18], pre-processing of image is needed to improve the calculation accuracy in image analysis process.

In this study, the influence of surface metallic particle on the tracking property due to successive flashover at $SF_6$/insulator interface was studied based on the analysis of FD. Flashover test was conducted on a basin-type insulator under DC voltage in $SF_6$ gas environment in a GIS bus subsection. Conducting particle was placed on the surface at various locations to study the influence of metallic particle on flashover property. Tracking due to successive discharge was captured. And then image analysis based on fractal theory was applied to calculate the FD of the tracking pattern. The quantitative relation between the FD of the tracking and the electric field distribution near the particle tip was discussed. Finally, the influence of field distribution referring to surface particle on tracking pattern and flashover characteristics was claimed.

## II. EXPERIMENTAL SETUP

### A. $SF_6$ GAS AND INSULATOR

$SF_6$ gas was supplied by Liming Research Institute of Chemical Industry Co. Ltd. with the purity of 99.99%. 420 kV basin-type insulators consisting of bisphenol-A epoxy resin as the matrix with aluminum oxide ($Al_2O_3$) micro-particles at 70 wt% as filler were prepared and supplied by Pinggao Group Co. Ltd. Image of the solid insulator is displayed in Fig. 1.

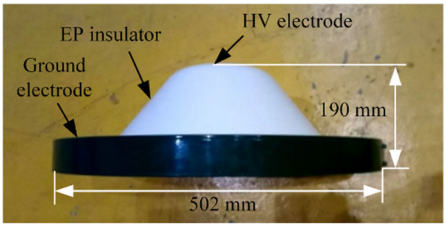


**FIGURE 1.** Image of basin-type epoxy resin insulator.

The copper particle with the diameter of 0.5 mm and the length of 25 mm was employed as the surface metallic particle. According to the report [19], the diameter of the typical metallic particles inside the GIS is several hundreds of micrometers. Thus, the diameter of 0.5 mm was selected. Besides, if the length is too small, flashover would occur in the path without metallic particle according to our previous investigation. This will lead to difficult in the investigation of tracking during successive flashover. Thus, the length of 25 mm was selected. According to the previous investigation of particle movement, the metallic particle would more likely attach to the middle region of the insulator surface after successive collisions. Thus, the copper particle was placed at 19, 71, 123 and 175 mm away from HV electrode respectively which provided quartered locations along the surface between HV and ground electrodes. Diagram referring to the relative location between insulator and particle is shown in Fig. 2.

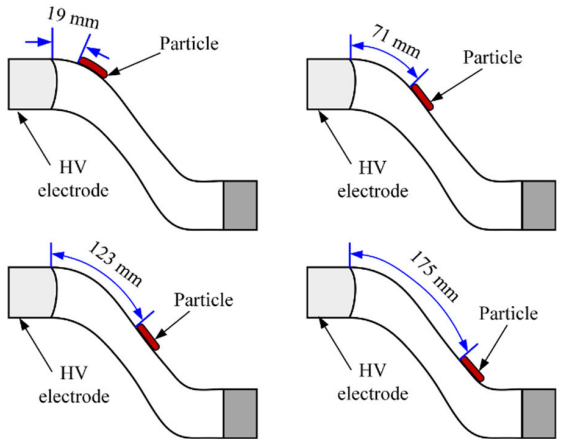


**FIGURE 2.** Diagram of the insulator with particle at various locations. The figure only shows the half part with particle.

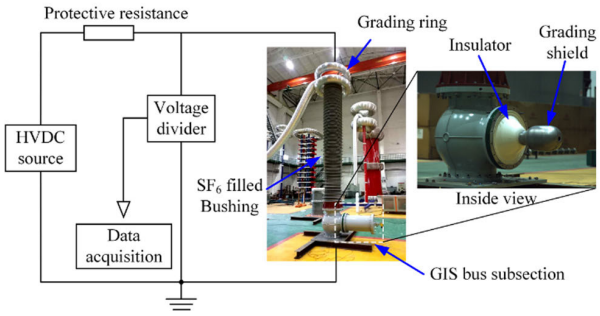


**FIGURE 3.** Experimental setups for surface flashover test.

### B. SURFACE FLASHOVER MEASUREMENT

DC flashover measurement system is shown in Fig. 3. The insulator was sealed in a 420 kV GIS bus subsection supplied by Pinggao Group Co. Ltd. whose HV side was connected to HVDC source. The surface of insulator was cleaned by ethyl alcohol and dried before fixed in the cell to prevent the influence of surface pollution. The cell was vacuumed to 30 Pa and then inflated with $SF_6$ gas up to 0.06 MPa. The whole system was standing for 20 min before the voltage was applied. Positive DC voltage provided by the source (ZDFI ±1200 kV supplied by Xinan Electrotechnics Co. Ltd.) was applied and increased at 1 kV/s until flashover occurred.

Each set of tests was repeated until 20 times of successive flashover were obtained with the same particle location. Flashover voltage was obtained and tracking after successive discharge was recorded by an HD camera. All the tests were conducted in room temperature.

## III. IMAGE ANALYSIS METHOD

### A. IMAGE PROCESSING

A typical image of tracking on insulator surface is illustrated in Fig. 4(a). The image is shown in 2D mode while actually the tracking followed the 3D shape of the insulator. This will result in shrink along radial direction in the captured image compared to the actual size of the tracking. In this article, image process procedure was operated to the original image for the purpose of achieving accurate result in following fractal analysis procedure.

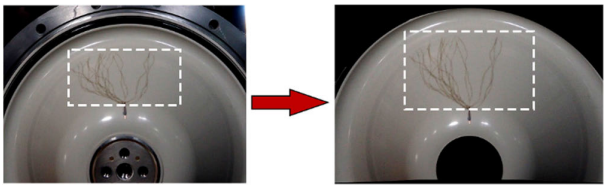


**FIGURE 4.** Illustration of image processing from original image to flatted image. (a) Original image, (b) Flatted image.

Distance between a certain point on the surface and HV electrode along insulator surface could be obtained once the structural of the insulator is given. Thus, a mapping relation can be established which deals with the distance from a point to reference point in captured image and the actual distance from the point to the reference point along insulator surface taking the center of HV electrode as the reference point. Each pixel in captured image could be converted with corresponding new coordinates as shown in Fig. 4. It can be observed that the area covered by tracking in Fig. 4(b) are larger than that in Fig. 4(a). In this way, original image can be flatted considering perspective effect and the structural of insulator.

### B. FD ALGORITHM

Fractal analysis is considered to function as a desirable approach to investigate discharge phenomenon which has already been applied to creeping discharge at liquid/solid interface [20], electric tree in transparent dielectrics [21] and discharge current signal [22]. Usually, box-counting method is used to calculate the FD of a binary image. Supposing an image with the size of $M \times M$ pixels, boxes with size of $r \times r$ pixels are prepared to cover all the effective pixels in the image, and the count of box can be obtained as $N(\mathrm{r})$ with varying the size of box. If the scatters $(\log(1/r), \log(N_r))$ are plotted on a figure with double logarithmic axes and then fitted with a straight line, the slope of the line is defined as the corresponding FD [22].

However, due to the random propagation path of discharge and irregular shape of the insulator, height and width of the image are arbitrary integers. Margin would remain uncovered with the size smaller than the length of the box when square boxes are applied to cover the entire image [23]. This will lead to calculation error. Thus, improved box-counting method should be introduced to improve the counting accuracy [23]–[25]. It is claimed the method suggested by So *et al*. is proved to show desirable accuracy and accessibility in fractal analysis [26], thus it was applied in this article to analyze the tracking property.

Briefly, for a given binary image with rectangle shape, square boxes are firstly applied to cover the effective pixels in the image in sequence as usual leaving the potential margin uncovered. Then the margin with the size smaller that the size of covering box is covered by cut-size box. In this procedure, the count of box needs to be weighted according to the ratio between the area of the cut-size box and full-size box. The total count of covering box is the sum of full-size box and cut-size box in the two counting procedures. Finally, the scatters corresponding to the count of box with vary the size can be plotted in double logarithmic axes and FD could obtained through line fitting.

## IV. RESULT AND DISCUSSION

### A. FLASHOVER VOLTAGE

Positive flashover voltage is illustrated in Fig. 5 with the particle at various locations. The voltage without particle can reach up to 354 kV and was significantly reduced as the consequence of surface conducting particle. It is obvious that the voltage increases with moving particle to ground electrode which is 179, 267, 296 and 312 kV for particle at 19, 71, 123 and 175 mm respectively. Flashover strength is reduced to half compared the voltage corresponding to particle at 19 mm and the voltage without particle.

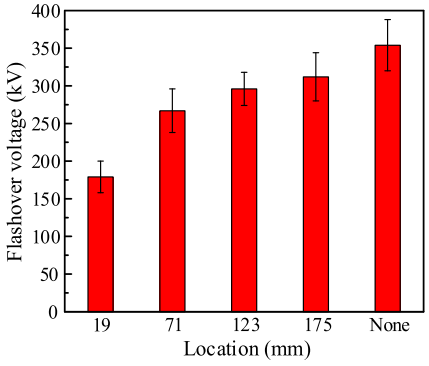


**FIGURE 5.** Relation between positive flashover voltage and particle location.

This implies that metallic particle in gas insulated system would cause severe discharge and voltage drop especially when the particle is adhered to insulator surface near HV electrode. Metallic particle would be charged and lift up under the stress of electrical field, then the particle will collide with the insulator and electrode which may lead to the adhering of particle to insulator surface at various locations. Thus, attention should be paid in particular on the influence

of particle location and focused on the improved method to prevent the corresponding damage due to discharge. Besides, it can be seen in this figure that the experimental deviation of flashover voltage lies in the range from 20 to 40 kV. With moving the particle towards the ground electrode, this deviation shows no increasing or decreasing tendency.

Flashover voltage variation could attribute to the field distortion due to the adhered particle which can be confirmed by simulation result. Finite element method was applied to simulate the field distribution concerning on the influence of conducting particle via ANSYS Maxwell module. The geometry model in this simulation is illustrated in Fig. 6. The length of the model is 1600 mm. The size of the insulator is corresponding to Fig. 1. The electric conductivity of the insulator and $SF_6$ gas was $1 \times 10^{-15}$ and $1 \times 10^{-19}$ S/m, respectively. The relative permittivity of the insulator and $SF_6$ gas was 4.95 and 1.002, respectively. The potential of the high voltage conductor and shielding was 420 kV. The enclosure was grounded whose potential was 0 V. The two boundaries of the model were electrically insulating.

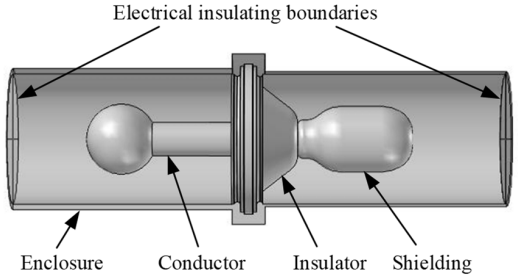


**FIGURE 6.** The geometry model in the simulation of electric field distribution.

Since the influence of voltage polarity on the electric conductivity of $SF_6$ gas and the insulator was neglected in this simulation, the simulation result of electric field distribution under 420 kV was the same as the result under −420 kV in amplitude. While the direction of the electric field lines was opposite. The result with respect to the electric field distribution would show no difference under different polarities. Thus, in this study, only the electric field distribution under 420 kV is provided. The block diagram of the simulation is shown in Fig. 7.

Results in Fig. 8(a) to (d) present the field distribution with particle at the location of 19, 71, 123 and 175 mm respectively. All these results in this figure are prepared in side view.

It is evident that conducting particle would significantly increase partial field strength, in particular, at the tips of particle with noticeable field distortion and extremely high value. For most part of the insulator, the field strength would not be changed much. Only the half with particle shows distortion while the other part without particle performs the field distribution lower than 5 kV/mm.

Field distributions in radial direction along the surface are illustrated in Fig. 9 for the particle at 19, 71, 123 and 175 mm,

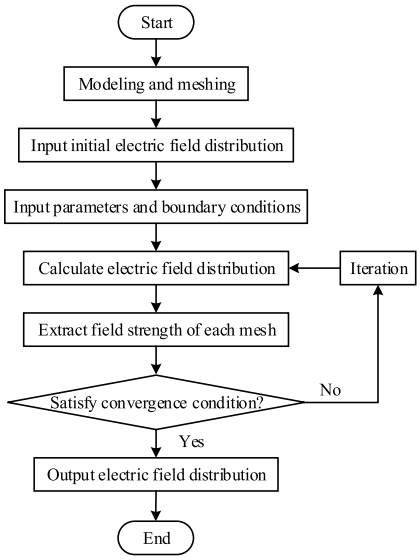


**FIGURE 7.** The block diagram of the simulation.

respectively, along with the field distribution without particle as the reference. The field strength increases up to 2.4 kV/mm in the middle and was reduced near HV electrode by the shield for the result without particle as shown in Fig. 9(a). However, it can be seen that there are apparent peaks at the tips of the particle with extreme high field strength which is far higher than the result without particle. Except for 19 mm, with moving the particle towards HV electrode, the peak becomes higher. The increase of partial field strength would lead to the increasing risk of initial discharge and finally result in the voltage drop of flashover.

According to the calculation of electric field distribution, the electric field strength at the tip of the particle is extremely high. This will cause serious ionization in the $SF_6$ gas near the tip under high voltage. And charged particles will be generated near the tip and diffuse to the surroundings. The path consisting of the charged particles shows excellent electric conductivity compared with the insulating gas. For the particle at 19 mm, once the path bridges the metallic particle and the electrode, the metallic particle can be regarded as the prolongation of the high voltage electrode attributing to the high conductivity path. The metallic particle can be regarded as an obvious protrusion of the high voltage electrode. This will lead to an obvious decrease of flashover voltage. When the metallic particle is placed away from the high voltage electrode, for example at 71 mm, it is difficult to obtain the high conductivity path consisting of charged particles. Since the path is too long for the charged particles to bridge the high voltage electrode and the metallic particle tip under diffusion effect. Thus, the flashover voltage with particle at 19 mm is the lowest.

### B. TRACKING PROPERTY

Images of tracking are illustrated in Fig. 10 for the particle at various locations. Obvious brown tracking remains on insulator surface at the half part of insulator with particle and

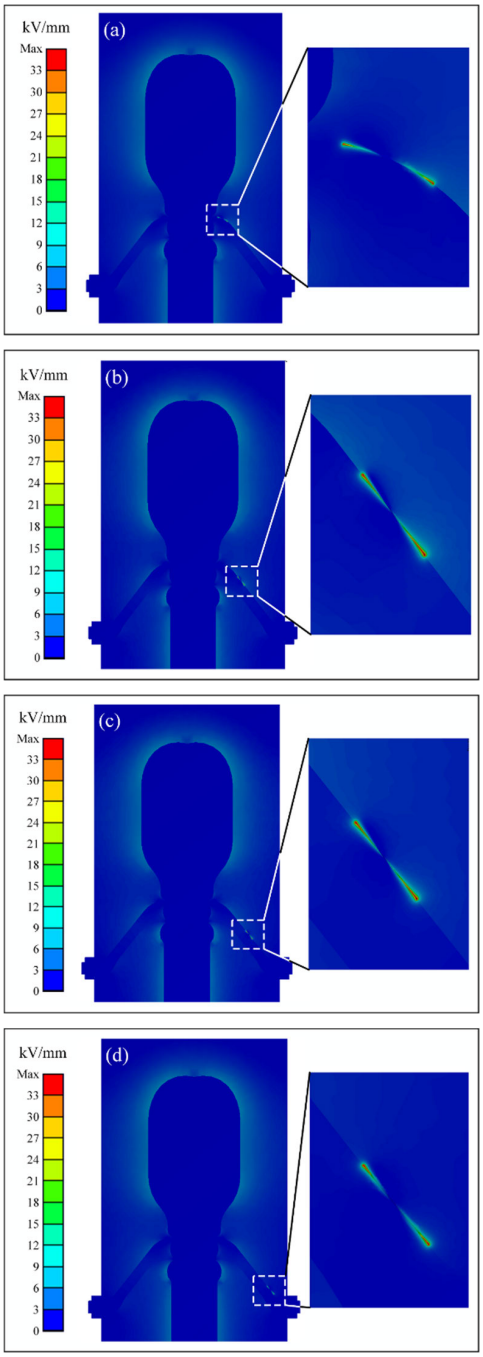


**FIGURE 8.** Field distribution of insulator in side view. From (a) to (d), the particle moves from HV electrode to ground electrode. The insert figure in each sub-figure shows the field distribution near the particle.

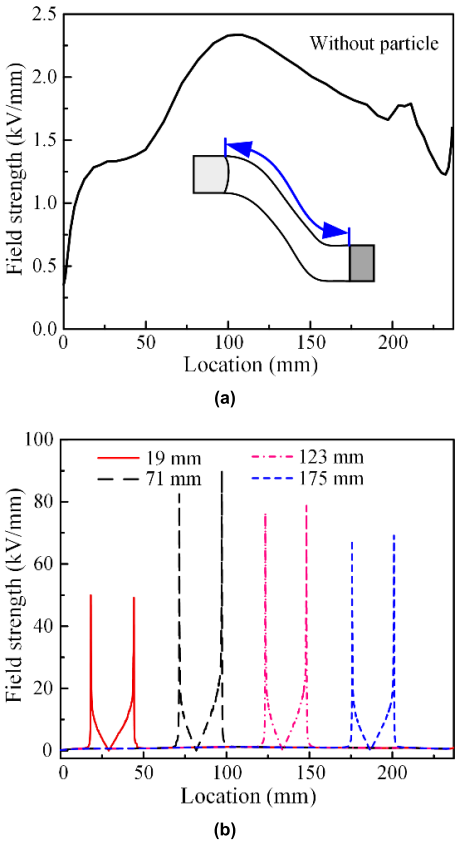


**FIGURE 9.** Field distribution along the surface in radial direction. (a) shows the field distribution without particle, (b) shows the field distribution with particle at various locations.

shows various patterns for different conditions. The tracking is divided into two parts which are the HV part covering the region from HV electrode to the tip of particle and the ground part covering the region from the tip of particle to ground electrode.

Regarding HV part, with moving particle from HV electrode to ground electrode, the area of tracking increases and the tracking pattern performs increasingly radial tendency. Meanwhile, ground part shows opposite pattern as the tracking performs centralized pattern with increasingly narrow region. Although HV part of 175 mm and ground part of 19 mm show similar tracking pattern with radial shape, there are obvious dark paths bridging the electrode and particle in 175 mm condition while the tracking shows perfect radial pattern in 19 mm condition. This could attribute to the fact that for HV part discharge will propagate across the area from HV electrode to particle tip in a path as short as possible at considerable possibility. Some of discharges would occur along this direction resulting in dark brown tracking on the surface during successive discharge.

For the tracking with particle at 19 mm, only the ground part shows obvious tracking while there is no obvious tracking in the HV part. Since the particle is placed near the HV electrode, the particle can be regarded as the prolongation of the electrode due to the ionization in $SF_6$ gas. The ground part bridging the particle and the ground electrode would dominate the discharge path. Thus, obvious tracking remains on the insulator surface as the consequence of successive surface discharge. Similar mechanism leads to the obvious tracking in the HV part with particle at 175 mm, while there is no obvious tracking in the ground part.

For the particle in the middle region of the surface, for example at 71 mm, the tracking with respect to HV part needs to bridge the particle tip and the high voltage electrode.

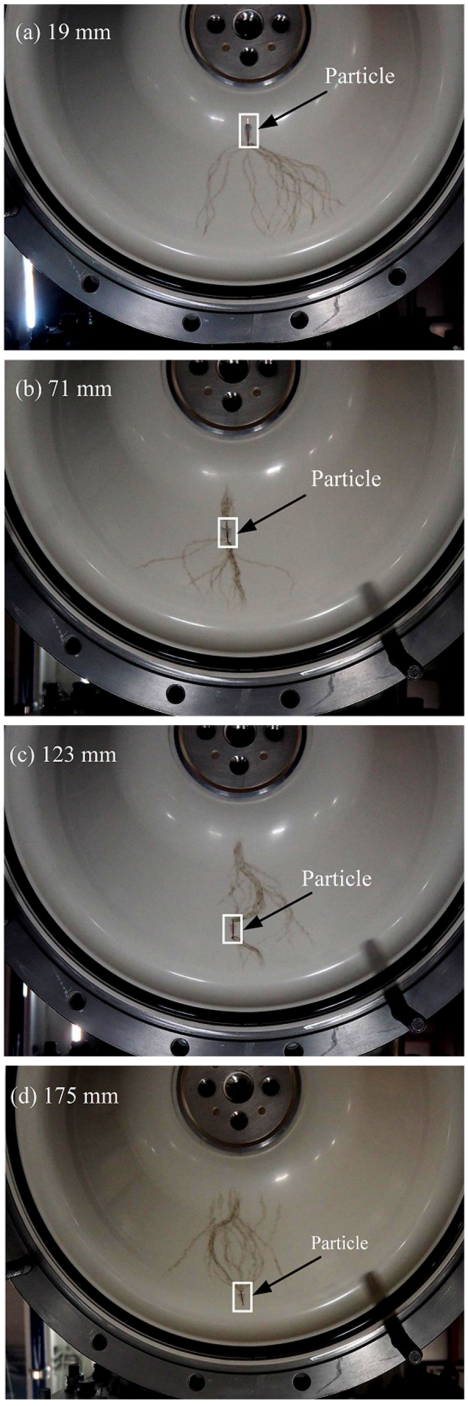


**FIGURE 10.** Images of tracking on insulator surface with the particle at various locations.

While the tracking with respect to ground part needs to bridge the particle tip and the ground electrode. As shown in Fig. 11, the potential area on the ground electrode (marked as Region 2) which acts as one end of the ground tracking is wider than the area on the high voltage electrode (marked as Region 1) which acts as one end of the HV tracking. Thus, the discharge path with respect to the Ground tracking has more choice than the HV tracking. Hence, the ground tracking shows more obvious radial pattern. Similar mechanism leads to the different tracking pattern at the two ends of the particle with the particle at 123 mm.

The dark brown tracking corresponding to successive flashover could lead to increasing risk of discharge as the consequence of increasing conductivity [13]. Thus, the propagation path with high probability may form the weak point in insulation. According to the result of ground part, particle location near ground electrode may result in serious damage via certain path on insulator surface as the consequence of centralized tracking. Meanwhile the location near HV electrode may cause damage with large area as flashover would occur in various direction covering a fan-shape region with approximate mean probability.

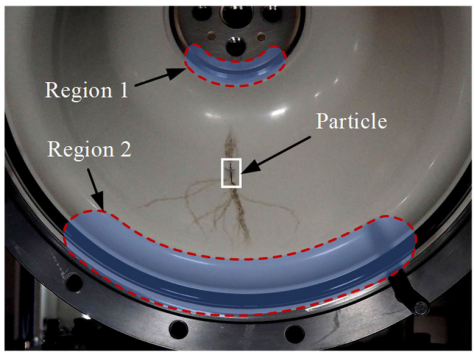


**FIGURE 11.** Potential area at electrodes acting as the ends of tracking.

To evaluate the tracking pattern, fractal analysis was introduced to estimate these images after processing as discussed above. FD of each image in Fig. 10 was calculated and shown in Fig. 12 according to the improved box-counting method. Since the tracking of ground part with the particle at 175 mm seems too fuzzy to recognize, FD of ground part only shows the results corresponding to the images in Fig. 10(a), (b) and (c). The same reason leads to the missing result of 19 mm for HV part.

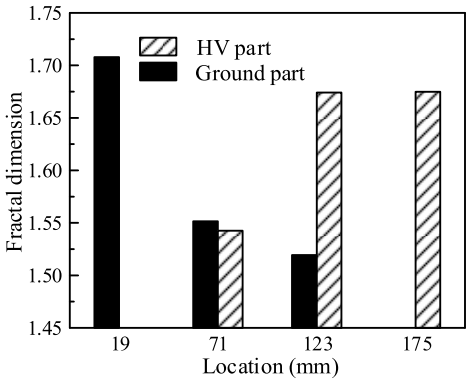


**FIGURE 12.** FD of the tracking on insulator surface with the particle at various locations.

As shown in Fig. 12, FD of ground part decreases with moving the particle to ground electrode, while FD of HV part increases with the same variation. For the branch network in

a two-dimension system, for example the tracking image in this study, the FD of this network varies from 1 to 2. The FD of a dash line is 1. And the FD increases with increasing area which is covered by the branch network. The FD approaches 2 when the branch network covers the entire two-dimension plane. Thus, the FD of a more radial pattern is high than the FD of a more centralized pattern. The higher FD of tracking indicates more obviously radial pattern as confirmed in Fig. 10(a) for ground part. The results imply considerable discrimination to evaluate the tracking pattern based on FD and indicates possible approach to diagnose the influence of particle on flashover property.

In order to reveal the potential influence on tracking pattern, field distribution was investigated and is shown in Fig. 13 via main view. Only the region with particle shows obvious field distortion while other parts performs relative low value. This may explain the phenomenon that only the half part with particle shows obvious tracking after successive flashover while there is not any tracking on the other half.

Field distribution along circle direction near ground tip of the particle was obtained and is illustrated in Fig.14 for further investigation dealing with the relation between field distribution and tracking pattern. The circle was set taking the center of HV electrode as the center point. The radius of the circle was 1 mm longer than the distance from center to the tip of particle as illustrated in Fig. 15. The results are shown with normalized location to obtain the same x-coordinate in the figure for different reference circles corresponding to the particle at different locations. Field strength was normalized since the absolute value of field strength, especially for the peak value, varies with various particle locations which though would perform vital influence on flashover voltage, however, shows slight effect on tracking pattern. The calculation of normalized location and field strength can be defined as (1) and (2),

$$L_n = \frac{L_r}{L_h} \tag{1}$$

$$E_n = \frac{E_r - E_0}{E_p - E_0} \tag{2}$$

where $L_n$ represents the normalized location along circle direction, $L_r$ represents the actual distance from the given point to start point along the circle and $L_h$ represents the length of half circle. $E_n$ is the normalized field strength, $E_r$ is the actual field strength at the point on the circle, $E_0$ is the reference field strength referring to the start point and $E_p$ is the peak field strength along the circle.

It is obvious that the field strength reaches the peak value at the angle to the tip for the particle at different locations. The distribution follows Normal-like distribution with a peak and sharply decreases at peak region and finally reaches a low value. Further, the peak region shows centralized tendency with moving the particle to ground electrode.

In order to investigate the relation between the electric field distribution at the particle tip and the tracking pattern, the field distribution characteristics at the tip were

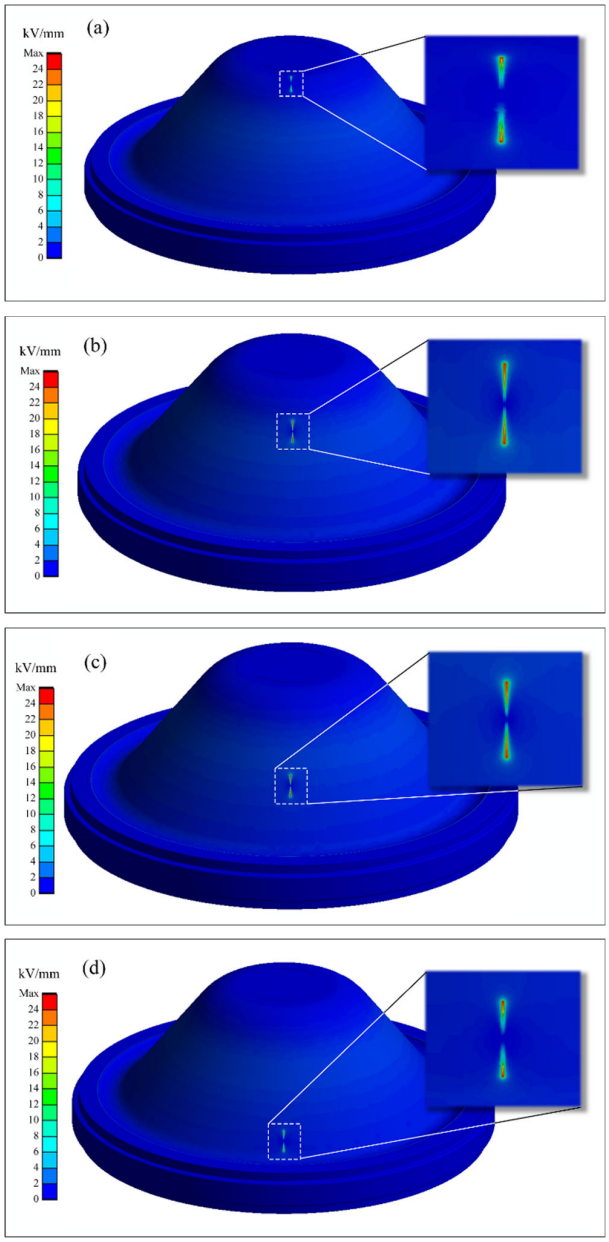


**FIGURE 13.** Field distribution of insulator in main view. From (a) to (d), the particle moves from HV electrode to ground electrode. The insert figure in each sub-figure shows the field distribution near the particle.

analyzed quantitatively. A fitting function with two Gaussian distribution terms was employed to fit this normalized electric field distribution. The fitting function is shown as follows:

$$F(x) = a_1 \times e^{-\left[\frac{(x-b_1)^2}{c_1^2}\right]} + a_2 \times e^{-\left[\frac{(x-b_2)^2}{c_2^2}\right]} \tag{3}$$

where $F(x)$ is the normalized field strength, $a_1$, $a_2$, $b_1$, $b_2$, $c_1$ and $c_2$ are fitting parameters, $x$ is the normalized location in Fig. 14. Among them, $b_1$ and $b_2$ represent the center location of the two curves corresponding to the two exponential terms while $c_1$ and $c_2$ describe the broad property of the peaks. The values of $c_1$ and $c_2$ are illustrated in Fig. 16 along with corresponding FD. Thus, the relation between the electric

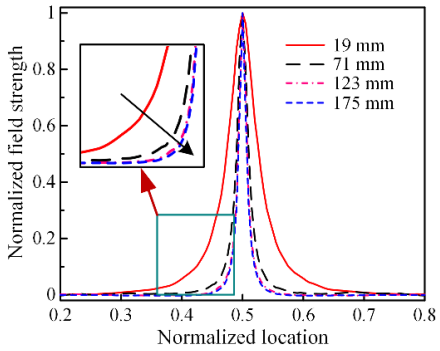


**FIGURE 14.** Field distribution along the surface in circle direction. The insert figure shows the field distribution near the peak.

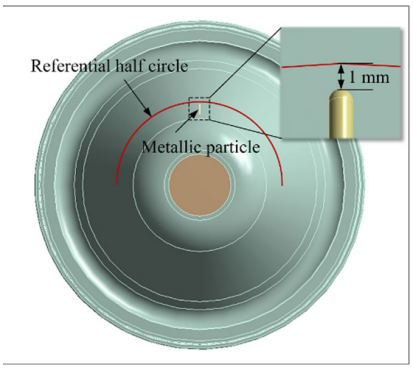


**FIGURE 15.** Schematic diagram for the calculation of field strength along circle direction. The red arc represents the reference half circle.

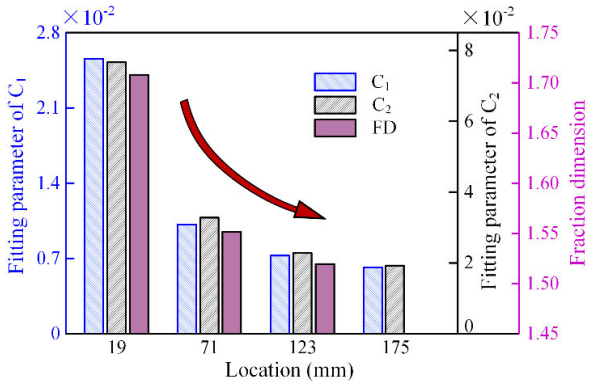


**FIGURE 16.** Relation between fitting parameters and FD with particle at various locations.

field distribution at the particle tip and the tracking pattern is revealed quantitatively.

It can be observed that $c_1$ and $c_2$ deceases with moving the particle to ground electrode following the similar tendency of FD. This indicates the significant influence of field distribution on flashover propagation characteristics. High field strength would increase the possibility of corona discharge leading to the initial partial discharge at certain region. More than peak point, it can be observed that the peak region near the tip shows high field strength compared to the region less influenced by the particle. The high field strength would contribute to the initiation of corona discharge however the location of particle is. It is expected that the wider peak region contributes to the higher probability for discharge propagating in radial direction. Finally, this leads to the various directions and paths for flashover propagation and results in the radial pattern of tracking after successive flashover.

Tracking would cause serious damage to surface insulation. Thus, investigation of tracking pattern would be benefit to evaluate the influence of metallic particle on the flashover characteristics with respect to the deterioration property of insulation. Since the tracking is the consequence of successive flashover, the tracking pattern indicates the probability of discharge path along the surface. Thus, this investigation reveals the quantitative relation between the discharge property and the particle property with the help of analyzing the tracking pattern and electric field distribution. This method can reveal the probability property with respect to the discharge path according to the quantitative analysis of tracking images. This method reveals the influence of surface metallic particle on the surface discharge characteristics which may be beneficial in the design of structure and selection of material. Also, it can help to improve the insulating performance of GIS/GIL with insulators.

Besides metallic particle, defects including crack, bubble and contamination would also result in initial discharge under operation voltage and finally contribute to flashover. The evaluation and analysis method suggested in this paper could be applied in the investigation of the discharge characteristics for these conditions. Meanwhile, tracking provides desirable advantage compared to flashover voltage in estimating insulating property and shows considerable information to identify flashover with off-line and easy-to-obtain properties.

## V. CONCLUSION

This article investigated the DC flashover property of basin-type insulator in $SF_6$ gas considering the influence of surface metallic particle. Tracking pattern due to successive discharge was analyzed based on fractal theory. The conclusion can be summarized as follows:

(1) Brown tracks remained on insulator surface due to successive flashover and the tracking was separated by the particle. Improved FD calculation method based on box-counting was suggested to analysis the tracking pattern considering the shapes of insulator and tracking.

(2) Tracking pattern of the ground part showed centralized tendency with moving the particle to ground electrode, and corresponding FD decreased. Quantitative analysis indicated that Normal-like field distribution near the tip dominated the centralized pattern and the variation of FD.

(3) FD analysis in this article claimed quantitative relation between tracking pattern and field distribution for HVDC insulator. Investigation on tracking pattern showed advantages of convenience and abundant information referring to flashover characteristics.

## REFERENCES


[1] H. Koch, *Gas Insulated Substations*. Chichester, U.K.: Wiley, 2014, pp. 50–52.

[2] H. Niu, Z. Chen, H. Zhang, X. Luo, X. Zhuang, X. Li, and B. Yang, "Multi-physical coupling field study of 500 kV GIL: Simulation, characteristics, and analysis," *IEEE Access*, vol. 8, pp. 131439–131448, 2020.

[3] Y. Xing, Z. Wang, L. Liu, Y. Xu, Y. Yang, S. Liu, F. Zhou, S. He, and C. Li, "Defects and failure types of solid insulation in gas insulated switchgear: *In situ* study and case analysis," *High Voltage*, to be published, doi: 10.1049/hve2.12127.

[4] Y. Gao, Z. Li, H. Wang, and X. Yuan, "Metal particle encouraged surface charge accumulation on epoxy insulator with multi-arc surface profile under DC voltage," *IEEE Trans. Dielectr. Electr. Insul.*, vol. 27, no. 3, pp. 998–1006, Jun. 2020.

[5] Y. Gao, H. Wang, X. Yuan, H. Zhao, and Z. Li, "Surface charge accumulation on a real size epoxy insulator with bouncing metal particle under DC voltage," *IEEE Trans. Plasma Sci.*, vol. 49, no. 7, pp. 2166–2175, Jul. 2021.

[6] B. Qi, C. Li, Z. Xing, and Z. Wei, "Partial discharge initiated by free moving metallic particles on GIS insulator surface: Severity diagnosis and assessment," *IEEE Trans. Dielectr. Electr. Insul.*, vol. 21, no. 2, pp. 766–774, Apr. 2014.

[7] Y. Xing, X. Sun, Y. Yang, G. Mazzanti, D. Fabiani, J. He, and C. Li, "Metal particle induced spacer surface charging phenomena in direct current gas-insulated transmission lines," *J. Phys. D, Appl. Phys.*, vol. 54, no. 34, Aug. 2021, Art. no. 34LT03.

[8] L. Zhang, C. Lin, C. Li, S. V. Suraci, G. Chen, U. Riechert, T. Shahsavarian, M. Hikita, Y. Tu, Z. Zhang, D. Fabiani, and J. He, "Gas–solid interface charge characterisation techniques for HVDC GIS/GIL insulators," *High Voltage*, vol. 5, no. 2, pp. 95–109, Apr. 2020.

[9] C. Li, J. Hu, C. Lin, B. Zhang, G. Zhang, and J. He, "Surface charge migration and DC surface flashover of surface-modified epoxy-based insulators," *J. Phys. D, Appl. Phys.*, vol. 50, no. 6, Jan. 2017, Art. no. 065301.

[10] J. Ma, Q. Zhang, H. You, Z. Wu, T. Wen, C. Guo, G. Wang, and C. Gao, "Study on insulation characteristics of GIS under combined voltage of DC and lightning impulse," *IEEE Trans. Dielectr. Electr. Insul.*, vol. 24, no. 2, pp. 893–900, Apr. 2017.

[11] L. Xing, L. Weidong, X. Yuan, C. Weijiang, and B. Jiangang, "Surface charge accumulation and pre-flashover characteristics induced by metal particles on the insulator surfaces of 1100 kV GILs under AC voltage," *High Voltage*, vol. 5, no. 2, pp. 134–142, Apr. 2020.

[12] L. Que, Z. An, Y. Ma, F. Shan, Y. Zhang, F. Zheng, and Y. Zhang, "High resistance of surface fluorinated epoxy insulators to surface discharge in $SF_6$ gas," *IEEE Trans. Dielectr. Electr. Insul.*, vol. 25, no. 1, pp. 245–252, Feb. 2018.

[13] Q. Xie, Y. Wang, X. Liu, H. Huang, C. Zhang, and T. Shao, "Characteristics of microsecond-pulse surface flashover on epoxy resin surfaces in $SF_6$," *IEEE Trans. Dielectr. Electr. Insul.*, vol. 23, no. 4, pp. 2328–2336, Aug. 2016.

[14] A. Beroual, M. L. Coulibaly, O. Aitken, and A. Girodet, "Effect of micro-fillers in polytetrafluoroethylene insulators on the characteristics of surface discharges in presence of $SF_6$, $CO_2$ and $SF_6$-$CO_2$ mixture," *IET Gener. Transm. Distrib.*, vol. 6, no. 10, pp. 951–957, Oct. 2012.

[15] F. Sadaoui and A. Beroual, "AC creeping discharges propagating over solid–gas interfaces," *IET Sci., Meas. Technol.*, vol. 8, no. 6, pp. 595–600, Nov. 2014.

[16] L. Kebbabi and A. Beroual, "Fractal analysis of creeping discharge patterns propagating at solid/liquid interfaces: Influence of the nature and geometry of solid insulators," *J. Phys. D, Appl. Phys.*, vol. 39, no. 1, pp. 177–183, Jan. 2006.

[17] Y. Lv, Y. Ge, Q. Du, Q. Sun, B. Shan, M. Huang, C. Li, B. Qi, and J. Yuan, "Fractal analysis of positive streamer patterns in transformer oil-based $TiO_2$ nanofluid," *IEEE Trans. Plasma Sci.*, vol. 45, no. 7, pp. 1704–1709, Jul. 2017.

[18] E. Volpov, "HVDC gas insulated apparatus: Electric field specificity and insulation design concept," *IEEE Elect. Insul. Mag.*, vol. 18, no. 2, pp. 7–36, Mar. 2002.

[19] Y. Xu, "Motion characteristics and partial discharge characteristics of submillimeter metal particles on the surface of AC GIS spacer," *Proc. CSEE*, vol. 39, no. 14, pp. 4315–4324, Jul. 2019.

[20] A. Beroual and V.-H. Dang, "Fractal analysis of lightning impulse surface discharges propagating over pressboard immersed in mineral and vegetable oils," *IEEE Trans. Dielectr. Electr. Insul.*, vol. 20, no. 4, pp. 1402–1408, Aug. 2013.

[21] B. X. Du, J. S. Xue, and M. M. Zhang, "Effect of pulse duration on electrical tree and breakdown process of epoxy resin in $LN_2$," *IEEE Trans. Dielectr. Electr. Insul.*, vol. 24, no. 1, pp. 359–366, Feb. 2017.

[22] I. Ramirez-Vazquez, J. Ruiz-Pinales, and J. Salgado-Talavera, "Fractal analysis of nano-reinforced silicone rubber insulators evaluated on a tracking wheel," *IEEE Elect. Insul. Mag.*, vol. 30, no. 4, pp. 21–27, Jul. 2014.

[23] J. Xu and G. Lacidogna, "A modified box-counting method to estimate the fractal dimensions," *Appl. Mech. Mater.*, vols. 58–60, pp. 1756–1761, Jun. 2011.

[24] Y. Kaewaramsri and K. Woraratpanya, "Improved triangle box-counting method for fractal dimension estimation," *Adv. Intell. Sys. Comput.*, vol. 361, pp. 53–61, 2015.

[25] M. Long and F. Peng, "A box-counting method with adaptable box height for measuring the fractal feature of images," *Radioengineering*, vol. 22, no. 1, pp. 208–213, Apr. 2013.

[26] G.-B. So, H.-R. So, and G.-G. Jin, "Enhancement of the box-counting algorithm for fractal dimension estimation," *Pattern Recognit. Lett.*, vol. 98, pp. 53–58, Oct. 2017.


**XIAOLONG LI** (Member, IEEE) was born in Fushun, China, in 1989. He received the B.S. and Ph.D. degrees in electrical engineering from Tianjin University, China, in 2012 and 2017, respectively. From 2018 to 2019, he was a Research Assistant with the University of Liverpool. He joined the Shenyang University of Technology, in 2017, where he is currently an Associate Professor. His research interests include gas discharge, electrical insulation and materials, modeling, and computer simulation.

**CHEN CAO** (Member, IEEE) was born in Liaoning, China, in 1987. He received the Ph.D. degree from the Shenyang University of Technology, in 2018. He is currently a Lecturer with the School of Electrical Engineering, Shenyang University of Technology. He is also with the Key Laboratory of Special Machine and High Voltage Apparatus, Ministry of Education. His research interests include fault diagnosis and online monitoring technology of the electrical equipment in the power systems.

**XIN LIN** (Member, IEEE) received the B.S., M.S., and Ph.D. degrees from Xi'an Jiaotong University, Xi'an, China, in 1982, 1985, and 1989, respectively. She is currently a Professor with the School of Electrical Engineering, Shenyang University of Technology, leading the research group on electric apparatus. She is the author/coauthor of more than 400 technical papers, more than 40 patents, and four books. Her research interests include high voltage apparatus, high voltage and insulation techniques, gas discharge, and its application in circuit breaker. She is the Director of CES and a member of CIGRE.